PROCEEDINGS, 51st Workshop on Geothermal Reservoir Engineering
Stanford University, Stanford, California, February 9-11, 2026
SGP-TR-230

Deploying Coiled Tubing Conveyed Fiber Optic Cables at the Utah FORGE Enhanced Geothermal System

Smith Leggett, Dan Keough, Aleksei Andriianov, Murtaza Rampurawala, Dana Jurick

807 Boston Ave, Lubbock, TX 79409

sleggett@ttu.edu

Keywords: DAS, DTS, RFS-DSS, distributed fiber optic sensing, DFOS, Utah FORGE, Instrumented Coiled Tubing, EGS

ABSTRACT

Fiber optic cables offer a powerful tool for monitoring enhanced geothermal systems (EGSs), and practical deployment approaches remain under development. We designed, tested, and field-deployed coiled tubing conveyed fiber optic cables to evaluate their feasibility for long-term, retrievable monitoring. The deployment was supported by benchtop strain testing and careful planning of coiled tubing operations. Operational lessons included the importance of circulation contingencies (e.g., burst discs), optimized blowout preventer stack height, and extended coil length at surface to aid in retrieval.

Distributed temperature sensing (DTS) measurements provided reliable bottomhole temperature estimates consistent with the bottomhole temperature gauge. Distributed acoustic sensing (DAS) indicated inflow zones and microseismicity. Standard single-mode fiber with RFS-DSS interrogation successfully captured thermal slug responses for production logging. The experimental strain-coupled fiber failed during installation, likely due to thermal expansion effects. Overall, this study demonstrates the feasibility of coiled tubing deployed fiber optics for retrievable monitoring in EGSs.

1. INTRODUCTION

Distributed fiber optic sensing offers multiple diagnostic measurements for entire wellbores in an enhanced geothermal system (EGS). At the Utah FORGE EGS field laboratory, distributed temperature sensing (DTS) in the 16B producer has been used to determine the geothermal gradient, characterize cement quality (Jurick 2023), and evaluate zonal isolation during stimulation (Jurick 2024). Well resolved temperature changes detected by Rayleigh frequency shift distributed strain sensing (RFS-DSS) have been interpreted to quantify the inflow distribution along the producer (Ou and Sharma 2025). During the stimulation campaign, the Utah FORGE team selected perforation intervals along the 16B at cross-well fracture intersection locations identified through RFS-DSS monitoring of the 16A stimulation (Jurick 2024). Distributed acoustic sensing (DAS) has also been used for microseismic monitoring and microseismic reflection imaging (Ma et al. 2025, Ma et al. 2026). Altogether, these measurements are valuable for characterizing important components of the EGS including the reservoir, wellbores, and stimulation processes and results.

Other distributed fiber optic sensing measurements have the potential to provide value for EGSs but have not been applied yet. Previous studies have demonstrated the use of DAS and RFS-DSS to estimate fracture widths in EGS reservoirs (Liu et al. 2021, Nwabueze and Leggett 2026). When combined with inter-well circulation volumes derived from chemical tracer tests, these measurements enable estimation of the fracture surface area available for heat exchange (Nwabueze and Leggett 2025).

Despite the benefits derived from fiber optic measurements, multiple fiber optic cable deployments have failed at the Utah FORGE site (Ajo-Franklin et al. 2025). At least one failure was attributed to a manufacturing defect, but most failures appear to have resulted from high-temperature environments and harsh operating conditions associated with stimulation and circulation activities. Fiber optic cable failures threaten the long-term utility of distributed fiber optic sensing in EGS wellbores. The EGS industry requires deployment methods that ensure the availability of valuable distributed measurements throughout the operational life of the EGS. Few studies have documented deployment strategies that prioritize the long-term survivability of distributed fiber optic sensing systems in high-temperature EGS environments.

Fiber-optic cable deployments in steam-assisted gravity drainage (SAGD) wellbores provide a relevant comparison for enhanced geothermal systems (MacPhail et al. 2016, Zaini and Keough 2017). Deployments typically occur in larger casing sizes, high-temperature environments, and deviated wellbores. There is a strong track record of successful fiber optic deployments in SAGD wells via a coiled tubing string (Kaura et al. 2008). In this work, we describe the design, deployment, and preliminary results of fiber optic cables installed within a coiled tubing string at the Utah FORGE site, drawing from design methods and experience gained from SAGD applications.

The following section describes the methods used to design and deploy the instrumented coiled tubing string.

2. METHODS

This section describes the design of the instrumented coiled tubing string and highlights benefits and limitations of the deployment relative to other deployment methods. It then describes benchtop laboratory experiments conducted to aid in selecting the silicone gel used in the

deployment of the strain-sensitive fiber. Next, we detail 16B wellhead modifications necessary for the deployment. Finally, the installation is described, with an emphasis on operational constraints and lessons learned.

2.1 Design of the Instrumented Coiled Tubing String

2.1.1 Sensor Selection

The design basis for the coiled tubing string consisted of several considerations and constraints. We required simultaneous measurement of DTS, DAS, and RFS-DSS. We hoped that the fiber used for RFS-DSS or low-frequency DAS strain sensing would be able to detect dilation and contraction of fractures during circulation operations. However, we anticipated that strain transfer from the formation to the fiber would be challenging and most probably, limited. Thus, we elected to install three separate 1/4-inch capillary tubes containing fiber optic cables. Two of the tubes connect at a turnaround sub as shown in Figure 1. These two tubes contain one single-mode fiber (SMF) and one multimode fiber (MMF) respectively. If one or both fibers deteriorate or fail, they can be retrieved by circulating specific fluids into one of the lines and retrieving the fibers out of the opposing line. Replacement fibers can be installed in a similar way. Another capillary tube containing one SMF and viscous silicone gel for enhanced strain transfer was constructed. Finally, a fourth 1/4-inch capillary tube is used as a tubing-encapsulated conductor (TEC) line for a bottomhole pressure and temperature sensor. The bottomhole temperature sensor provides a calibration point for the DTS measurement. The bottomhole pressure sensor eliminates the need to infer bottomhole pressure from surface measurements and enables measuring the bottomhole pressure falloff when the fluid level decreases from the surface.

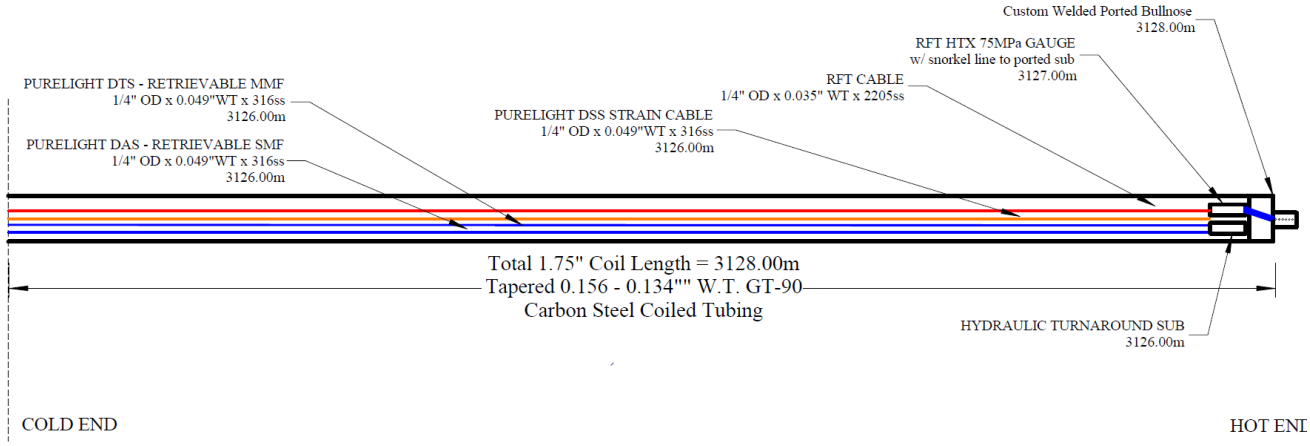

Figure 1: The 1.75-inch outer diameter (OD) coil tubing string incorporates four 1/4-inch capillary tubes. These include: (1) a tubing-encapsulated conductor (TEC) line communicating with a resonant frequency transducer (RFT) for pressure and temperature measurement; (2) a single-mode fiber (SMF) embedded in silicone gel for enhanced distributed strain sensing; and two pumpable and retrievable optical fibers in nitrogen, (3) one SMF and (4) one multimode fiber (MMF).

2.1.2 Coil Tubing Design

When selecting the diameter of the coiled tubing, we considered the number of instrument lines, equipment availability from the coiled tubing service provider, the desire to maximize the annular flow area to minimize frictional pressure losses, and the need for sufficient stiffness to deploy the coil into the deviated portion of the 16B wellbore. A 1.75-inch outer diameter coiled tubing was selected with a tapered wall thickness. The tapered wall thickness maximizes the strength of the coil at the upper section of the string, where most of the load is carried, while minimizing unnecessary weight at the bottom of the string.

The coiled tubing string is closed-ended and contains air around the capillary tubes. Wellbore fluids are not intended to enter the coil. The only exception is that ports are located along the bull nose at the end of the coil to enable hydraulic communication with the bottomhole pressure gauge. In the design phase, we considered installing a burst disc to enable communication if desired (for example, to circulate clean if the coil gets stuck), but because of time constraints and uncertainty as to the additional risks this might cause, this idea was not implemented.

Benefits of the coiled tubing deployment relative to permanent behind-casing or wireline installations include: 1) reduced risk for exposure to wellbore fluids, which should improve survivability; 2) the ability to deploy the fiber in deviated wells without tractor technology that might be temperature limited; and 3) the ability to replace damaged fibers without a workover. On the other hand, the coiled tubing reduces the wellbore flow area, thereby increasing frictional pressure losses of the circulation fluid. It also prevents other tools (wireline logging tools, perforation guns, etc…) from being run without a significant risk of wireline entanglement and becoming stuck. There is also reduced physical strain coupling to the geologic formation relative to a behind-casing installation. Figure 2 shows photographs of the manufactured coiled tubing string.

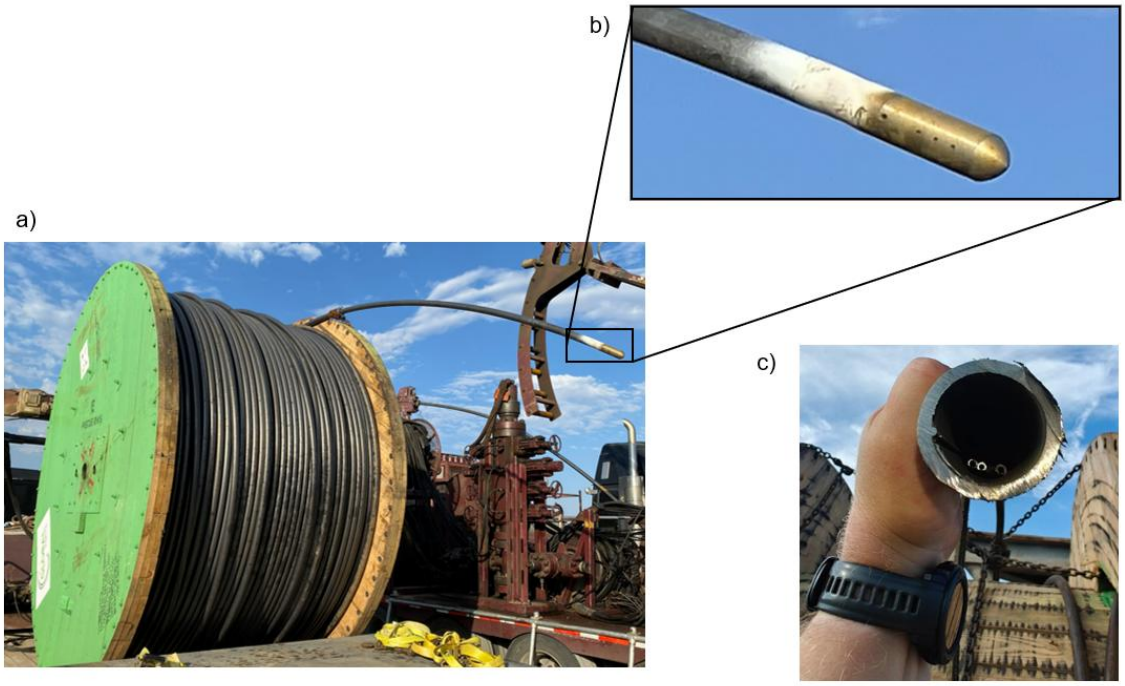

Figure 2: The instrumented coiled tubing string a) on the reel at Utah FORGE, with b) a closeup of the ported bull nose end to allow hydraulic communication to the downhole pressure gauge, and c) a cutaway of the coiled tubing string.

2.1.3 Enhanced Strain Sensing Cable

This section describes efforts to enhance the strain sensitivity of the third fiber optic cable. To detect fracture dilation and contraction, deformation must transmit to the SMF through the cement sheath, production casing, coiled tubing string, and the 1/4-inch capillary tubing string. Previous studies in horizontal shale wells have demonstrated that frictional coupling between production casing and wireline-deployed or pump-down fibers is sufficient to detect deformation of reservoir rock (LeBlanc et al., 2022). Using unconventional shale wells as an analogue, this study investigates the potential to sense fracture dilation and contraction with an instrumented coiled tubing string in the deviated sections of the 16B. To pursue this objective, strain transfer from the 1/4-inch capillary line to the optical fiber was enhanced by deploying the fiber in a silicone gel.

Thixotropic gels such as Sepigel are often used to fill tubes containing optical fiber for protection and enhanced strain transfer. However, gels typically used in shale oil and gas sensing applications do not maintain desired properties at higher temperatures. Accordingly, we conducted benchtop experiments at elevated temperatures to screen candidate gels for suitability under Utah FORGE subsurface temperature gradient conditions. As shown in Figure 3, a stepper motor drives a worm gear with a die to apply a load to a portion of a cable. The temperature is measured at thermocouple locations underneath an insulating heating blanket (not shown), while the strain along the fiber optic cable is recorded. Displacements are correlated with measured strain for a fiber with near-perfect strain coupling, and deviations from perfect coupling are observed for fibers in tubes with different gels. Detailed results are outside the scope of this paper, but a gel was selected that maximized strain transfer without compromising fiber integrity.

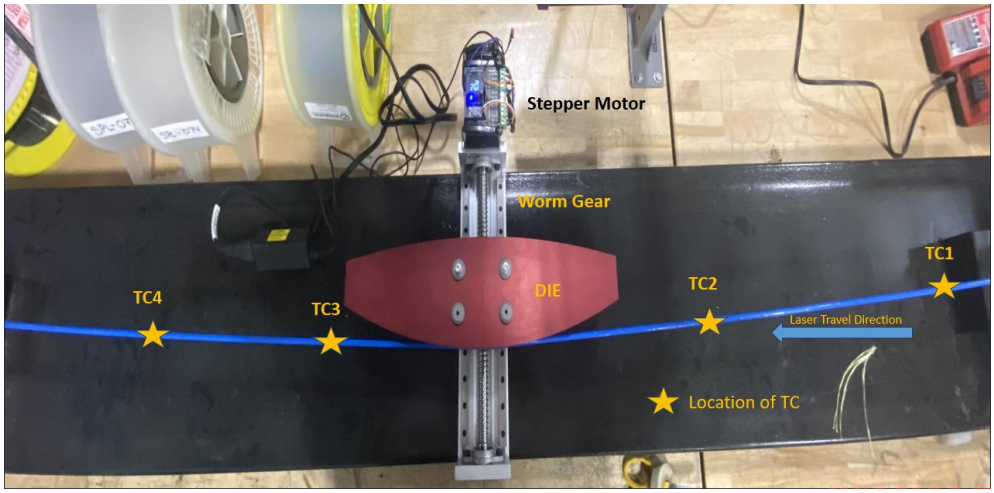

Figure 3: Benchtop strain transfer test rig to characterize the ability for candidate gels to enhance strain transfer to the optical fiber in the strain-sensitive 1/4-inch capillary tube.

2.2 Wellhead Modification

We modified the wellhead configuration of the 16B to land the coiled tubing for long-term monitoring. As shown in Figure 4, a flowcross was installed on top of the 7-1/16-inch master valve with two nominally 3-inch gate valves. On top of the flowcross, a 4-1/16-inch spool containing a slip and seal assembly was installed to enable hanging the coiled tubing. The maximum pressure rating of the flowcross and hanger assembly is 3,000 psig for temperatures from 0 to 350 °F, derated to 2,145 psig for temperatures above 350 up to 650 °F.

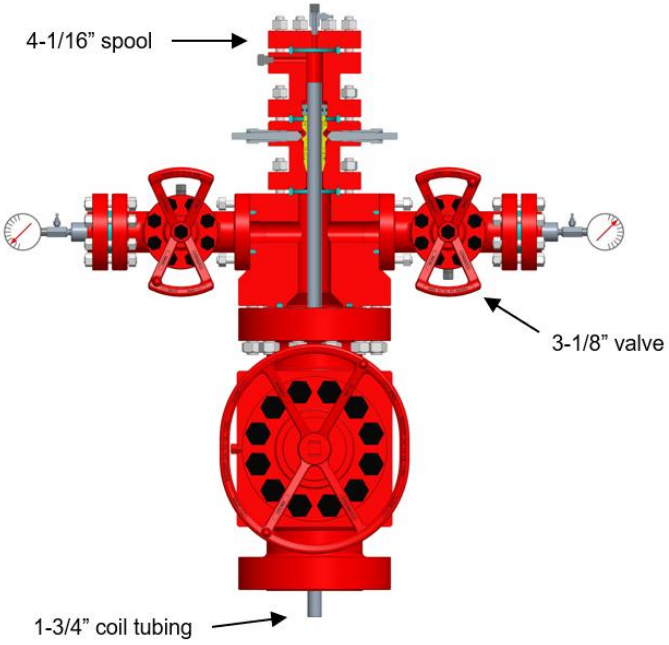

Figure 4: Wellhead modification of the 16B to land and hang the coiled tubing for long-term monitoring.

2.3 Installation

Figure 5 shows photographs of installation operations. A 110-ton crane was used to support the weight of the injector and gooseneck, approximately 11,000 lb., as well as the weight of the coiled tubing in the hole before it was landed. The top of the injector was approximately thirty feet above ground level. The height of the wellhead stack could have been reduced by decreasing the number of adapter spools between the coiled tubing hanger and the blowout preventer (BOP). The reservoir management team at Utah FORGE elected not to inject kill fluid into the well. Therefore, a work window was necessary to deploy the coiled tubing into the 16B with

approximately 100 psig of surface wellhead pressure. Once the coil reached the desired depth, the BOPs were closed, and the pressure between the stripper and the BOP was bled off. An operator on a manlift opened the work window, providing access to the coiled tubing, and inserted slips around the coil. The work window was closed, the BOP was reopened, and the coil was lowered until the slips landed in the wellhead hanger.

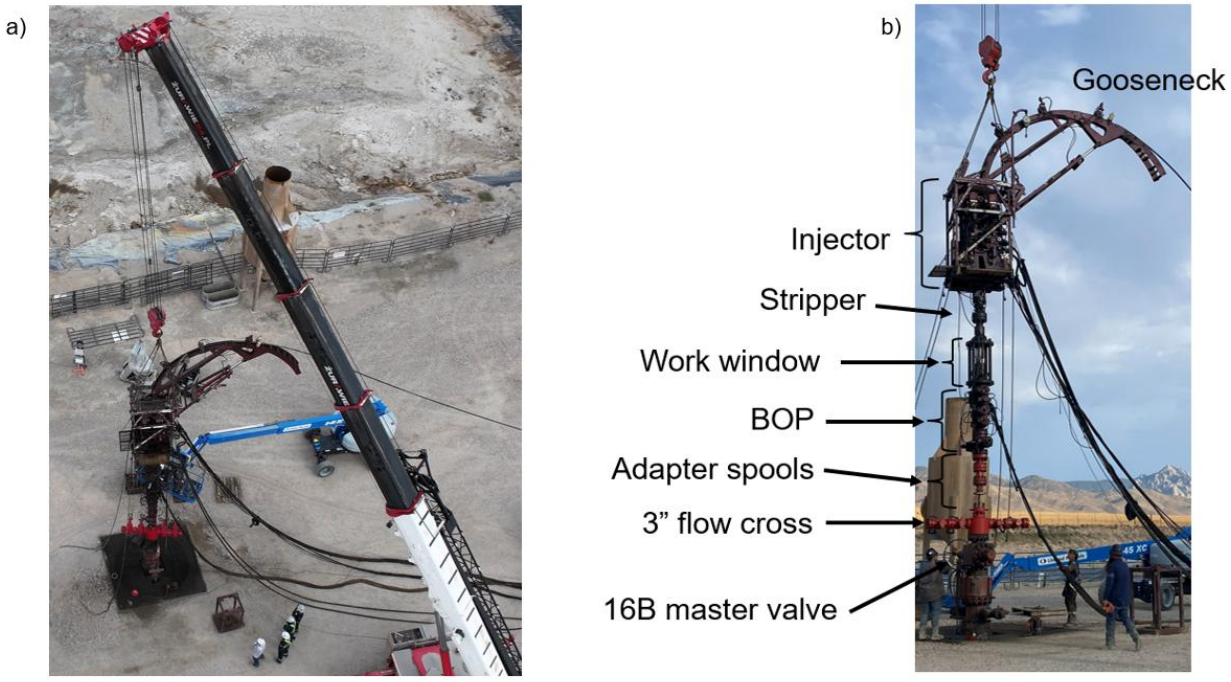

Figure 5: a) Aerial photograph of the 110-ton crane and wellhead assembly, b) labeled wellhead assembly.

Thecoiled tubing was landed at 10,100 feet measured depth. This depth was sufficient to cover all perforated intervals (deepest perforation at 9,773-feet) while remaining safely above the open hole section (open hole begins at 10,208-feet). The service company running the coiled tubing had the capability to digitally log multiple time series during the operation including depth, weight, and injector pressure. However, only the weight was logged digitally during the operation; depth was tracked manually.

As shown in Figure 6, between approximately 4:30 and 5:30 PM, the weight indicator readings departed from their trend, indicating a restriction. The operators used a manual depth indicator to manage the installation. Depths were referenced (zeroed) to the bottom of the stripper shown in Figure 5. Engineers in the coiled tubing control unit console manually noted the depths corresponding to significant events on the weight indicator. The coiled tubing operator worked the string up and down twice to pass through restrictions encountered between approximately 9,580 feet and 10,010 feet. These depths overlap with multiple perforation intervals stimulated in the 16B, suggesting the possibility of accumulated debris (possibly sand) in the wellbore.

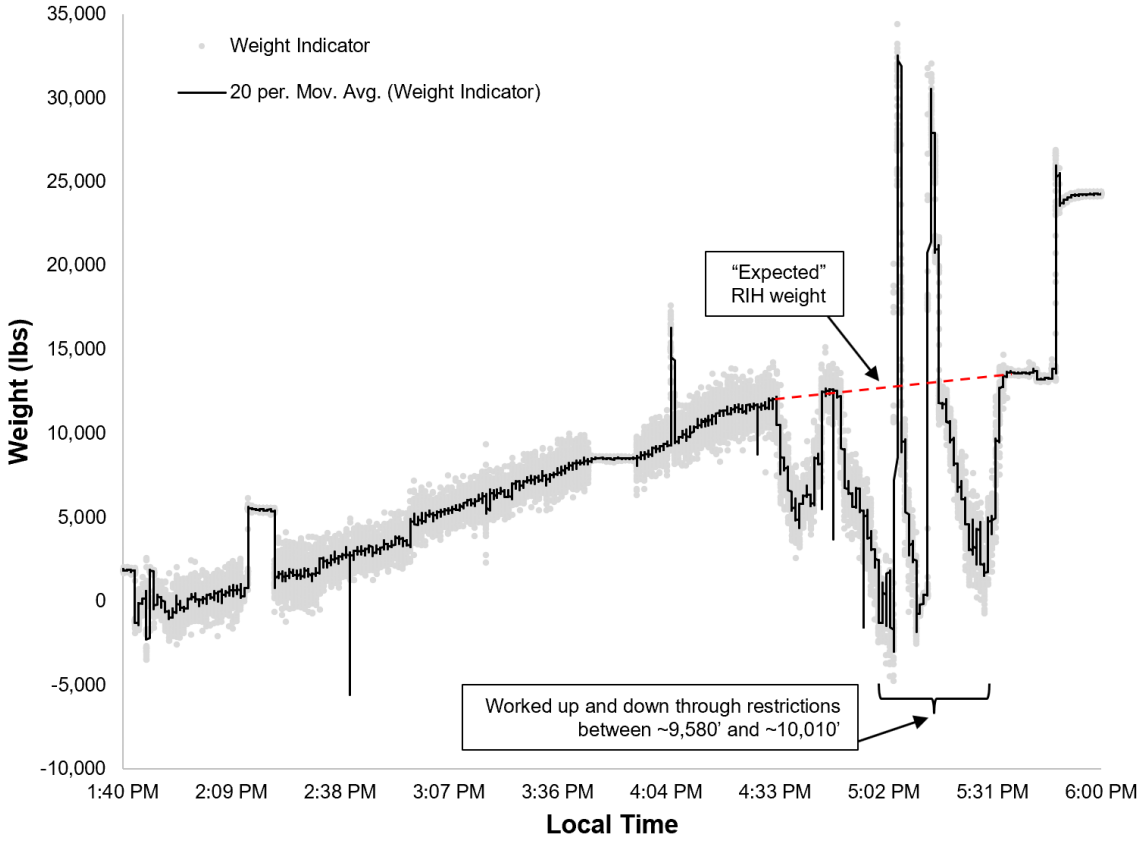

Figure 6: Weight indicator readings (with a 20-second moving average) during the coiled tubing installation. Departures from the trend indicate restrictions in the wellbore overlapping with perforated intervals.

After landing the coiled tubing in the hanger, operators cut off the excess length of the coiled tubing, removed the wellhead stack (everything above the flowcross and coiled tubing hanger), and demobilized the coiled tubing unit. The wellhead service provider installed the top spool, and Precise DHS organized the capillary tubing lines and terminated the optical fibers and the TEC line in a surface junction box for later access for interrogation. Figure 7 shows the final wellhead configuration.

Figure 7: Final 16B wellhead configuration.

The coiled tubing string can be removed from the 16B with a similar operation to how it was installed. However, this requires cutting the capillary tubing lines and welding or cold rolling a portion of another coiled tubing string to the one that is landed. Thus, each time the coiled tubing string is pulled and re-run, the usable length reduces. Discussions with the coiled tubing service provider suggest a best practice of leaving at least six inches of coiled tubing protruding from the hanger to facilitate a reconnection to the coiled tubing unit.

The next section presents measurement results from the instrumented coiled tubing acquired during subsequent EGS reservoir characterization experiments.

3. RESULTS

Immediately after the coiled tubing was landed, all optical fibers had strong readings to the end of the coiled tubing. However, the next day, the strain-sensitive fiber exhibited severe loss downhole near the kickoff point interpreted as a break in the fiber. Figure 8 shows an optical time domain reflectometry (OTDR) trace of the strain sensitive fiber following the failure. The OTDR depth axis in this plot is zeroed to a surface junction box, not the wellhead. The severe optical power loss at 6,890 feet (2,100 meters) represents a suspected break at approximately 6,368 feet (1,941 meters) from surface.

The root cause of the break is outside the scope of this publication, but we hypothesize that the break was related to the manufacturing process. The original intent was to fill the entire length of the strain sensitive fiber capillary tubing with silicone gel. However, friction from pumping the viscous gel into the 1/4” tubing resulted in approximately the bottom one-third of the tubing containing gel. The remainder of the capillary tube contained a mixture of nitrogen and air. The location of the fiber failure coincides with the suspected nitrogen-silicone gel interface. We speculate that thermal expansion of the silicone gel may have contributed to the break at this location. Unlike the SMF and MMF in capillary lines connected with a turnaround sub, this fiber is not retrievable. New methodology for manufacturing and strengthening fiber members will be utilized in future cases.

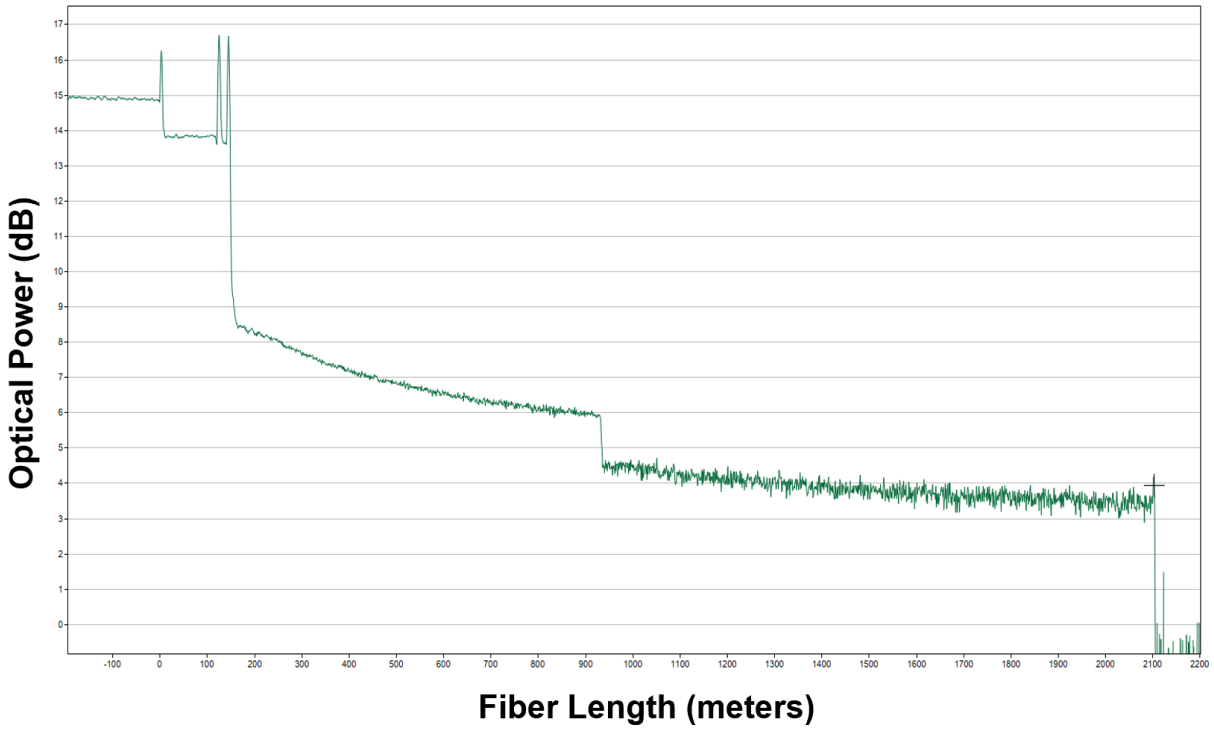

Figure 8: Optical time domain reflectometry (OTDR) trace showing failure of the strain-sensitive fiber at approximately 2,100 m (6,890 feet), relative to a surface junction box, corresponding to a subsurface depth of 1,941 meters (6,368 feet).

After the coiled tubing installation, researchers performed a one-week circulation test followed by an injection-flowback test at the Utah FORGE site. In the circulation test, brackish water was injected into the 16A and produced from the 16B. In the injection-flowback test, the brackish water was injected into the 16B and produced back. While a detailed analysis of these experiments is outside the scope of this paper, we highlight selected results from the instrumented coiled tubing string to demonstrate its utility. Neubrex Energy Services supplied the interrogators and managed all fiber optic sensing data acquisition and storage of the fiber optic measurements. Precise DHS installed a junction box with a data logger to record the bottomhole temperature and pressure.

Figure 9 shows DTS temperature measurements recorded on the retrievable multimode fiber. Below the waterfall plot, the bottomhole pressure and temperature as measured by the bottomhole gauges are displayed for comparison. The seven-day circulation test occurred between August 18 and August 25, 2025. Geothermal production warmed the wellbore during this period. The injection flowback test lasted four days and occurred between August 26 and August 30, 2025. Injection intervals are cool, immediately followed by warm production events. These observations demonstrate that DTS measurements using the MMF in the coiled tubing string capture thermal responses associated with operations in the EGS well.

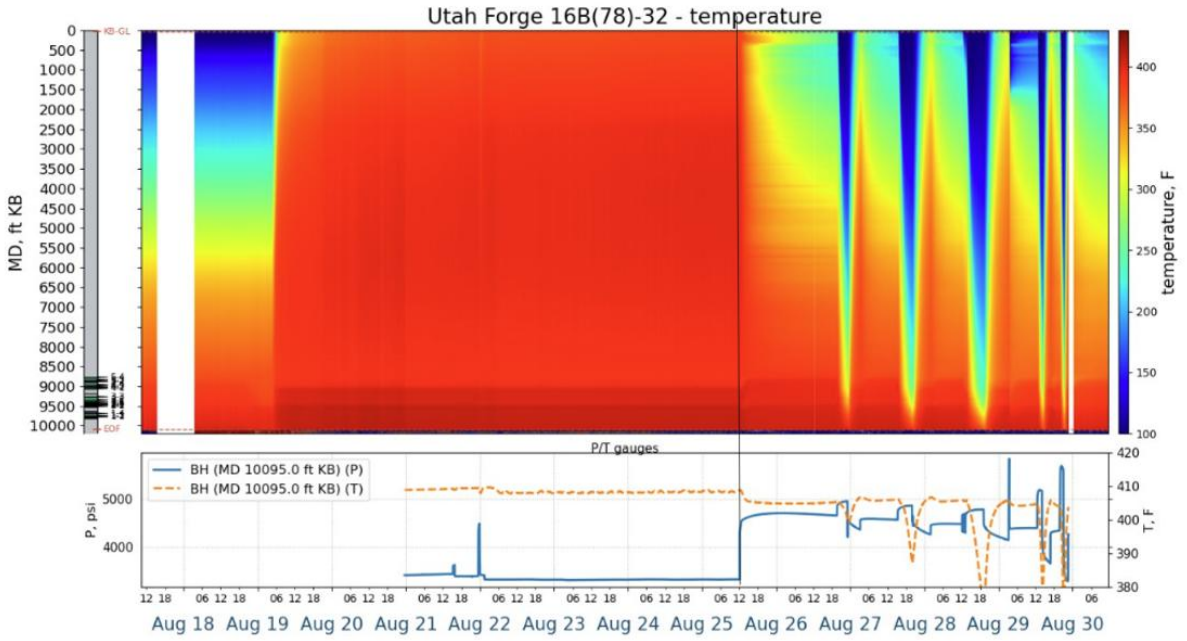

Figure 9: Overview of DTS measurements displayed as a waterfall plot from data measured on the retrievable multimode fiber during the circulation and injection-flowback operations.

Figure 10 displays Rayleigh frequency shift-based strain rate measurements recorded on the retrievable single-mode fiber. Time is on the x-axis, depth is on the y-axis, and the colors are presented as strain rate in units of microstrain per time interval (30-second profile interval). Although the units are presented as a strain change, RFS-DSS is sensitive to temperature change as well. We interpret that the measurements are primarily responding to temperature changes in the wellbore. The results can be interpreted as a time derivative of the DTS plot in Figure 9, but presented in microstrain unit scale. Larger temperature changes are observed during the injection-flowback test than during the circulation test. However, because of the 30-second acquisition speed along the entire fiber length, 20-centimeter spatial resolution, and 0.1 °C sensitivity to thermally driven strain changes of the RFS-DSS measurements, these data contain useful thermal slugging signals during the circulation test.

A surface choke downstream of the 16B wellhead provided backpressure on the well. When the choke size was changed, thermal transients were induced in the wellbore, one of which is illustrated in Figure 11. These thermal transients can be used to determine an inflow distribution or production log along the 16B (Nakamoto and Leggett 2025, 2026)

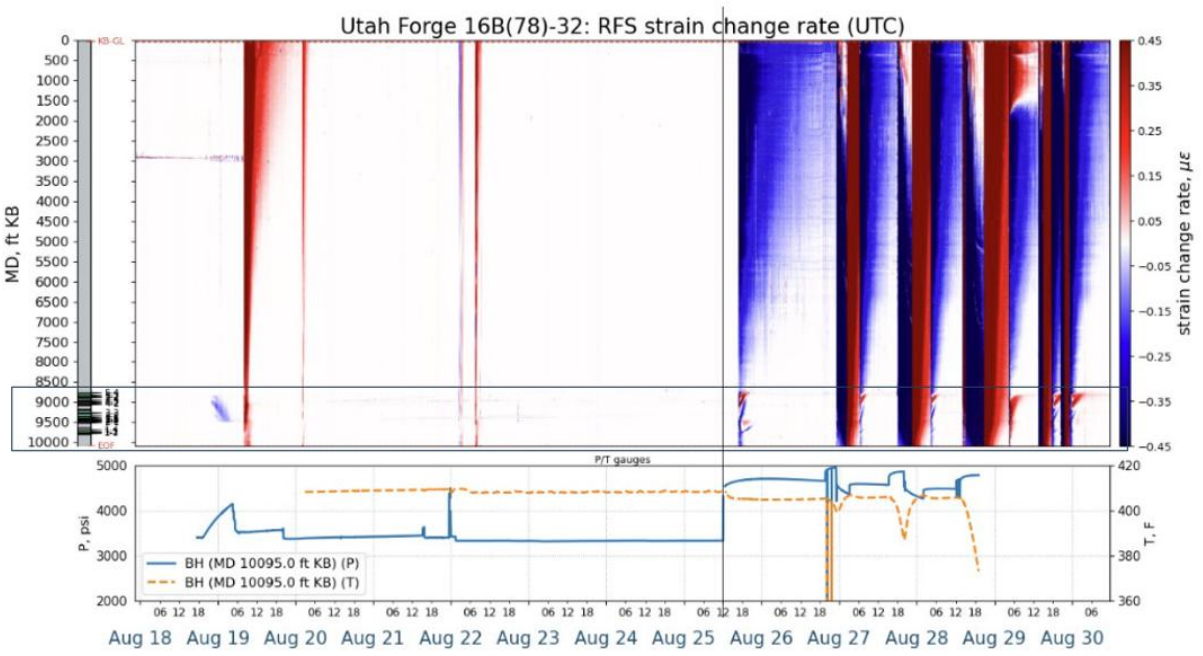

Figure 10: Overview waterfall plot of RFS-DSS strain rate measurements acquired on the retrievable single-mode fiber within the coiled tubing during the circulation and injection-flowback operations.

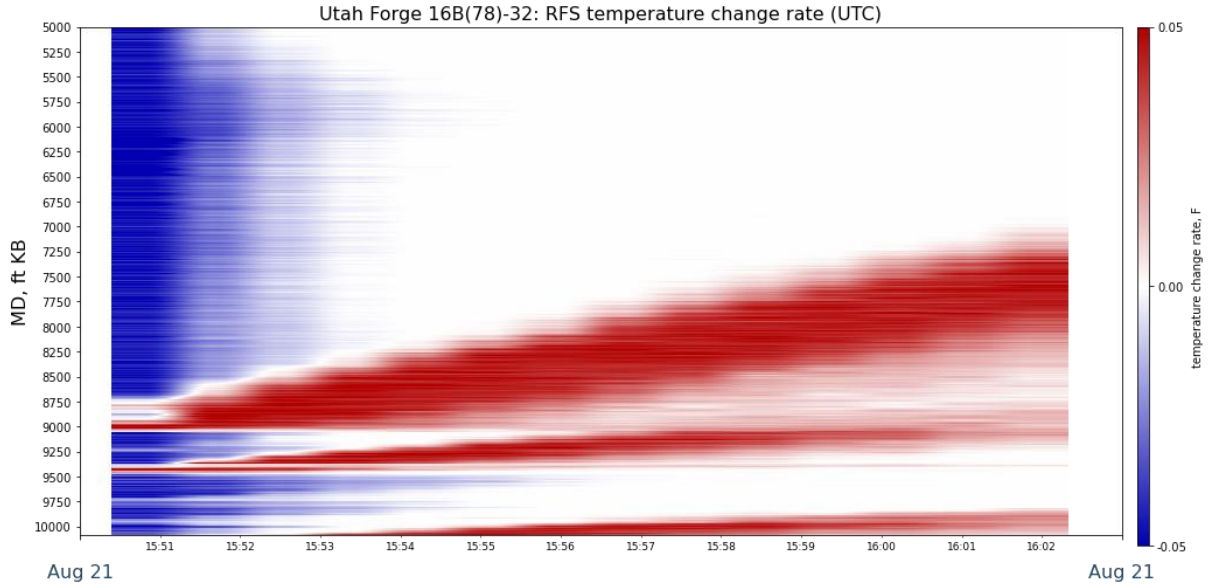

Figure 11: Example of an RFS-DSS-derived thermal slugging event in the 16B induced by surface choke adjustments.

The original plan was to acquire Distributed Acoustic Sensing (DAS) data on the retrievable single-mode fiber and RFS-DSS on the strain-sensitive fiber. Because of the failure of the strain-sensitive fiber, we recorded both RFS-DSS and DAS on the retrievable SMF using wavelength division multiplexing (WDM). WDM allows two or more interrogator units operating at different wavelengths to simultaneously probe the same fiber. DAS measurements were acquired from 0 to 4000 Hz during the entire acquisition period using Neubrex DAS interrogator. Figure 12 displays the DAS-measured frequency band energy (FBE) from two separate frequency ranges during one portion of the circulation test. The distance on the y-axis is the length along the fiber, including surface cable length, not

subsurface measured depth. As such, the horizontal bands between 9,700 and 10,000-feet fiber length on both plots occur within the 16B's perforation intervals. The elevated FBE responses at these locations are interpreted as acoustic noise induced by the circulation test.

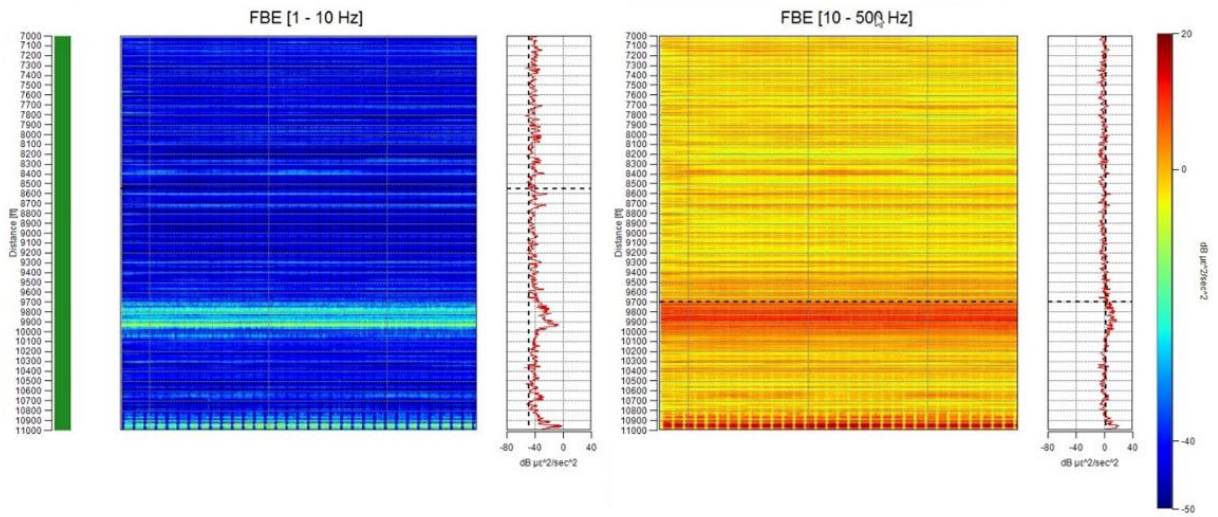

Figure 12: Example of noise recorded on DAS on the retrievable single-mode fiber during the circulation test.

DAS on the retrievable SMF also detected clear microseismic events. Figure 13 shows one such event that was measured during offset stimulation activities from an offset operator. This event occurred after the circulation and injection-flowback tests were completed and had a high signal to noise characteristic. This example demonstrates that broadband DAS measurements acquired through retrievable coiled tubing are sensitive to microseismic events despite significant mechanical decoupling from the formation.

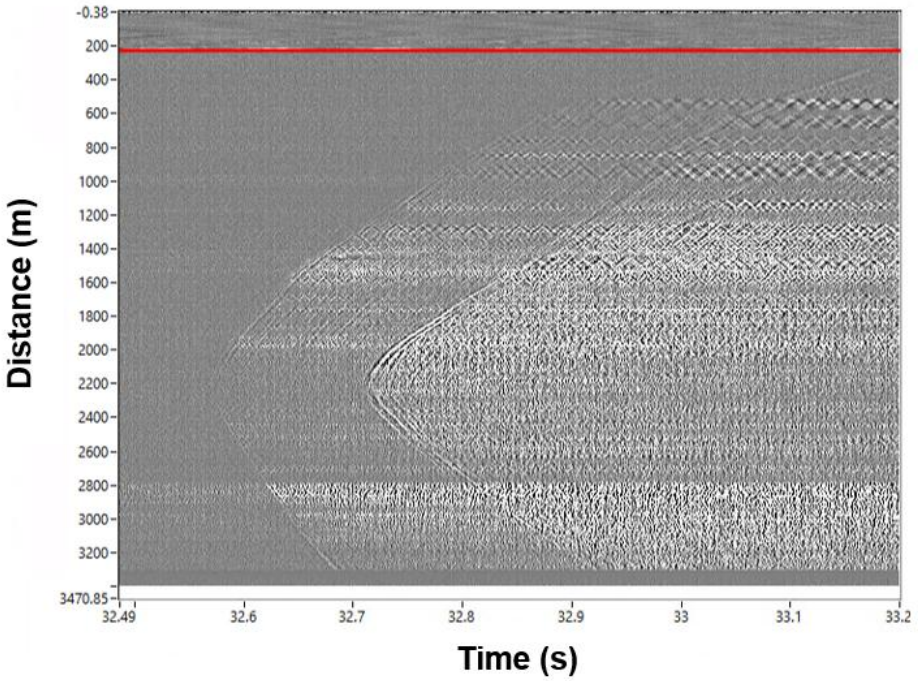

Figure 13: Example of a DAS microseismic event recorded on the retrievable SMF during offset stimulation activities from offset operator activities. Compressive (P) and Shear (S) wave arrivals are clearly visible over long sections of the fiber optics deployed in the coiled tubing. Shallow sections of the fiber response can be seen to have poor coupling characteristics, as evidenced by the zig-zag patterns in the DAS signal.

CONCLUSIONS

A fiber optic instrumented coiled tubing was deployed inside of casing in the 16B production well at Utah FORGE. Along with surface interrogator units connected to the fibers within the coiled tubing, the system provided valuable measurements of strain, temperature and microseismicity during and after circulation experiments, injection-flowback tests, and offset stimulation operations. It is notable that the DAS acquisition system acquired useful microseismic data with a high signal-to-noise ratio through multiple layers of a wellbore completion (fiber, nitrogen, capillary tubing, coiled tubing, casing, and cement). Deviation of the wellbore allowed physical coupling of the instrumented coiled tubing to the inside of the casing string and supported the acquisition of high quality RFS DSS, DTS and Acoustic data for data processing, analysis and interpretation. The strain-sensitive fiber provides another example, along with other compromised fibers at Utah FORGE, of the challenges associated with achieving strong strain coupling for distributed strain sensing in EGS environments. The installation experience resulted in important lessons learned, including:

1. The need to ensure the design of the coiled tubing hanger allows sufficient coiled tubing to protrude to facilitate a connection to the coiled tubing unit for future string retrieval;
2. A recommendation to consider including a burst disc in the coiled tubing string to enable circulation if the string becomes stuck;
3. A reminder to ensure the coiled tubing unit service provider digitally records both weight and depth as a time series during installation.

Strain coupled fiber optic deployment needs further work and trials, because availability of such data is critical for better understanding hydraulic fracture strain dynamics during short period circulation tests and for gaining understanding of the long term evolution of hydraulic fractures during the full life cycle of the circulation system.

ACKNOWLEDGEMENTS

This material is based upon work supported by the Department of Energy, Office of Energy Efficiency and Renewable Energy (EERE), under Award Number DEEE0007080.

In addition, the authors would like to acknowledge the support of the Utah FORGE team in planning and executing the experiment, including but not limited to: John McClennan, Kevin England, and Leroy Swearingen.

REFERENCES

Ajo-Franklin, Jonathan, Becker, Matthew, Charmarczuk, Michal et al. 2025. Distributed Fiber-Optic Sensing Deployment in a Deep EGS Production Well at Utah FORGE: Early Results and Lessons Learned (in English). *Stanford Geothermal Workshop*.

Jurick, Dana. 2023. *Utah FORGE: Neubrex Well 16B(78)-32 Cementing and Circulation Fiber Optics Monitoring Reports - July, 2023* trans. Wayne Fishback, Neubrex Energy Services (US), LLC (Reprint). https://gdr.openei.org/submissions/1559.

Jurick, Dana. 2024. *Utah FORGE: Neubrex Well 16B(78)-32 Stimulation and Circulation Fiber Optics Reports - Summer, 2024*, Neubrex Energy Services (US), LLC (Reprint). https://doi.org/10.15121/2448100.

Kaura, Jiten, Sierra, Jose, and Park, Bob. 2008. New High-Temperature Optical Fiber Technology Successfully Provides Continuous DTS Data under Severe SAGD Conditions. Presented at the SPE Asia Pacific Oil and Gas Conference and Exhibition. https://doi.org/10.2118/114458-MS.

Liu, Yongzan, Jin, Ge, Wu, Kan, and Moridis, George. 2021. Hydraulic-Fracture-Width Inversion Using Low-Frequency Distributed-Acoustic-Sensing Strain Data Part II: Extension for Multifracture and Field Application. *SPE Journal* **26** (05): 2703-2715. https://doi.org/10.2118/205379-PA.

Ma, Yuanyuan, Ajo-Franklin, Jonathan, Chamarczuk, Michal, Patterson, Jeremy, Zhu, Rosie, Vera Rodriguez, Ismael, Podrasky, David, Coleman, Thomas, and Maldaner, Carlos. 2025. Illuminating Geothermal Reservoir Structure: DAS Microseismic Reflection Imaging at Utah FORGE (in English). *Stanford Geothermal Workshop*.

Ma, Yuanyuan, Ajo-Franklin, Jonathan, Chamarczuk, Michal et al. 2026. Geothermal Reservoir Characterization at Utah FORGE Using DAS Microseismic Imaging. *Journal of Geophysical Research: Solid Earth* **131** (1): e2025JB032603. https://doi.org/10.1029/2025JB032603.

MacPhail, Warren, Kirkpatrick, James, Banack, Ben, Rapati, Bryan, and Asfouri, Alex Ali. 2016. SAGD Production Observations Using Fiber Optic Distributed Acoustic and Temperature Sensing: "SAGD DAS - Listening To Wells to Improve Understanding of Inflow". Presented at the SPE Canada Heavy Oil Technical Conference. https://doi.org/10.2118/180726-MS.

Nakamoto, Rion and Leggett, Smith. 2025. Development of a Transient Wellbore Heat Transfer Model Validated with Distributed Temperature Sensing Data. *Sensors* **25** (21): 6583. https://www.mdpi.com/1424-8220/25/21/6583.

Nakamoto, Rion and Leggett, Smith. 2026. An Analytical Approach to Production Logging in Enhanced Geothermal Systems Using Distributed Fiber Optic Thermal Slug Tracking. *Geothermics.* (Under review).

Nwabueze, Queendarlyn A. and Leggett, Smith. 2026. Proppant consolidation and hysteresis in hydraulic fractures: Insights from the application of a strain transfer model for interpreting fracture width changes from distributed fiber optic strain sensing. *Geoenergy Science and Engineering* **256**: 214159. https://www.sciencedirect.com/science/article/pii/S2949891025005172.

Nwabueze, Queendarlyn and Leggett, Smith. 2025. Application of Strain Transfer Model for Fracture Conductivity Modeling and Monitoring of Enhanced Geothermal Systems (in English). *Stanford Geothermal Workshop*.

Ou, Yuhao and Sharma, Mukul M. 2025. Estimating the Inflow Distribution in Geothermal Wells During Fluid Circulation Using Distributed Fiber Optic Measurements. *Proc.*, SPE Hydraulic Fracturing Technology Conference and Exhibition. https://doi.org/10.2118/223584-MS.

Zaini, Faiz and Keough, Daniel. 2017. Downhole Remote Monitoring System for SAGD Observation Wells through Fiber Optic DTS. Presented at the SPE Canada Heavy Oil Technical Conference. https://doi.org/10.2118/185006-MS.